

DETERMINATION OF ELONGATIONAL STRAIN DURING INK-ON-PAPER TACK MEASUREMENT: a novel technique to measure work of cohesion and adhesion of thin films

J. Schoelkopf
Group Leader
Surface Chemistry Research

P.A.C. Gane
Vice President
Research and Development

S. Fischer
Senior Scientist

Omya AG
CH 4665 Oftringen
Switzerland

ABSTRACT

In a previous paper we proposed a model of uniaxial extension to describe the viscous deformation of an offset-ink film on paper during ink-on-paper tack measurement as analysed on the Ink-Surface Interaction Tester (ISIT¹) (Gane *et al.*, *Proceedings Tappi IP&GA 2000, Savannah*). This now forms the subject for direct experimental confirmation. An optical reflection device based on a diode laser beam is used as a motion sensor to obtain data for the extensional rate of strain, $\dot{\epsilon}$. The application of the sensor requires that it have a resolution of approximately 1 μm and be able to record movement over a millisecond timescale. The motion of the tack wheel contacting a pre-printed surface is transferred via its extended axis to a thin connected mirror, pivoting around a fixed base-point. The laser beam acts as a pointer monitoring this displacement at a distant plane, where the position of the laser dot is recorded by means of a high speed digital camera. The collected data show a motion of quasi-linear acceleration, and hence strong extensional flow. The discontinuity at the start of the motion, during which any inertial effects arising from the initial short timescale acceleration, is limited to less than $\sim 1\%$ of the overall motion. This verifies the assumption made in the previous work, and, as a result, it is proposed that the experimental design encompassed by the ISIT can be used to evaluate the uniaxial extensional viscosity of relatively viscous fluids and pastes which show the necessary adhesional properties to a given substrate. Furthermore, the evolution of viscosity of such fluids can be monitored as a function of time, for example during concentration on contact with an absorbing porous medium. The case of ink-on-paper tack is used to exemplify the possibility to determine the work of extension during cohesive failure, i.e. the work of tack. The implications for boundary contact

adhesion are also discussed in terms of the measurement of the work of adhesion failure, if it occurs, during concentration of the ink at maximum tack levels.

Keywords: paper coating, ink tack, printability, elongational viscosity, strain sensor, thin film rheology

INTRODUCTION

During the print process the ink experiences pressure-induced shear and several stages of film splitting where cavitation and filamentation can occur. The breaking length of the filaments depends on the "shortness" of the ink, a phenomenological term which is important for the printer. In order to achieve a level glossy ink film the microscopic levelling of the broken filaments is crucial. Under conditions of poor levelling an often recognisable orange peel effect (more well-known in the context of paper filmpress coating) can be seen. Levelling can happen weakly under the influence of gravity on slow single colour presses, but usually more strongly due to spreading forces if the surface energy of the substrate is high enough (1) and due to the elastic relaxation of the induced film split roughness (6). The process is retarded with growing viscosity or tack as a result of fluid loss and viscous structure re-build, via substrate absorption and rearrangement of the interactive polymer components respectively. This results eventually in a decreasing thickness of the mobile ink layer, but the phenomenological effect of tack build-up at the early stages of absorption can be related to the viscous properties of the ink during fluid loss.

We previously analysed the viscous dependency of tack by combining independent rheological measurements on inks at different solids contents with the force-time relationship of the ISIT pull-off force (2), which probes the time dependent tack development of an ink film setting on a paper. The static pull-off mode of the ISIT is designed to provide a close approximation to a constant acceleration extensional regime. This feature is part of the machine control system defined by the ramp-down function of the applied solenoid contact force, and is confirmed independently here by direct observation of the tack wheel motion. Defining the rheological extensional regime requires knowledge of the evolution of strain. Previously we derived equations containing an a priori unknown term for the extensional strain, $\dot{\epsilon}$, so as to make a first

¹ ISIT is a product name of SeGan Ltd., Perrose, Lostwithiel, Cornwall PL22 0JJ, U.K.

approximate prediction. Our aim here is to determine the strain rate by direct observation. The outcome helps to verify the earlier made assumptions about the general form of separation via a thin ink film, and continues to support the viscous-related theory of the tack force components present during the cohesive tack measurement prevalent in the early stages of tack development on paper, though the previous assumption of a constant viscous response in the force-time integral can no longer be supported (2). The analysis can now be taken further to show that the response of the ink to shear is, as predicted by independent rheological observation, time and strain rate related, and that the work of tack and of adhesion at maximum tack can thus be derived.

THEORY

The basic physics behind the tack force has been previously described (3). The now classical interpretation of the ISIT measurement technique, involving optical examination of the pull-off areas on the printed paper stripe and the tack force curve over time, proposes a rupture at the weakest point of the adhesion/cohesion chain between the substrate, the thin ink film and the blanket-like tack wheel (4).

In respect to ink wetting and adhesion, it should be mentioned that the surface tension of an ink is not easy to measure because of its low mobility. Although the surface tension of the typically present mineral oil is quite low, the ink itself has a strong contribution from the more polar binders, their solvating agents, e.g. linseed oil, and the relatively high surface energy of the suspended solid particles. Formation of an extended lamellar filament of ink would, in principle, give information involving the surface energy.

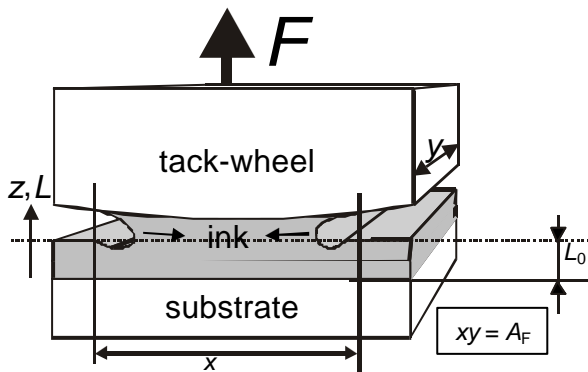


Fig. 1 Schematic view of tack measurement set-up under extensional separation.

Corresponding to Fig. 1, a more comprehensive model was introduced by the authors (2) as follows in the general form of:

$$F = F_{ad} + F_m + F_L + F_{cav} + F_{\zeta} + F_i$$

Eq. 1

where F is the force measured on one single pull-off and the subscripts denote the single components contributing to that force: from left to right - adhesion, meniscus tension, Laplace "underpressure" in the liquid phase, cavitation, viscosity and inertia. While all the components were considered as partial contributors, the most important component was identified as F_{η} . However, this "viscous" force under extension in fact relates back also to the surface energy as menisci are formed, and when high also invokes the adhesion to the substrate and tack wheel. Therefore, the measured force F forms the renewed subject for the following discussion.

Let us consider an uniaxial extensional term as, for example, given by the strain expression \mathbf{e} (5), in which the extension of the applied layer under test to a dimension of L occurs from a start dimension of L_0 :

$$\mathbf{e} = \ln(L/L_0)$$

Eq. 2

such that the uniaxial extensional viscosity, \mathbf{h}_u , can be expressed via the stress tensor, T_{ij} ,

$$\mathbf{h}_u = (T_{zz} - T_{yy}) / \dot{\mathbf{e}} = \frac{F(t)e^{\dot{\mathbf{e}}t}}{A_F \dot{\mathbf{e}}}$$

Eq. 3

where \mathbf{e} is the Hencky strain. To obtain an expression without the unknown rate of change of strain, Eq. 3 can be integrated with respect to time over the complete single pull-off curve using $F(t)$ as the measured separating force acting over a footprint area A_F to obtain a process extensional viscosity, \mathbf{h}_{pu} .

$$\frac{\int_0^{\infty} F(t) dt}{A_F} = \int_0^{\infty} \mathbf{h}_{pu} \dot{\mathbf{e}} e^{-\dot{\mathbf{e}}t} dt = \left[-\mathbf{h}_{pu} e^{-\dot{\mathbf{e}}t} \right]_0^{\infty} = \mathbf{h}_{pu}$$

Eq. 4

The ISIT software provides directly the force-time integrals, so \mathbf{h}_{pu} , can be obtained directly confirming earlier intuitively proposed relationships (4).

The values can now be matched with an extrapolated independently determined viscosity $\mathbf{h}^*(0)$ of the ink (at the relevant solids content (2)) taken from relaxation studies after shear. If, as a first approximation, the Trouton ratio is assumed, then using

$$\mathbf{h}_{\text{pu}}(t) = 3\mathbf{h}_1(t)$$

Eq. 5

we can relate the extensional viscosity to the shear viscosity. Our earlier study then normalised $\mathbf{h}_1(0)$ with $\mathbf{h}^*(0)$ by an arbitrary scaling factor, k .

The assumptions implicit in the integration made in Eq. 4 include that the effect of changing L_0 is ignored and that L is large when T_s represents the time at the end of the pull-off, i.e. that $\dot{\mathbf{e}}$ is large as the tack wheel finally extends the ink to fracture point, and therefore separation. The argument used previously was that if this assumption were true the boundary of the integral in t can be considered as $t \approx \infty$. If this were not the case then Eq. 4 would become,

$$\frac{\int_0^{T_s} F(t) dt}{A_F} = \int_0^{T_s} \mathbf{h}_{\text{pu}} \dot{\mathbf{e}} e^{-e\dot{\mathbf{t}}} dt =$$

$$\left[-\mathbf{h}_{\text{pu}} e^{-e\dot{\mathbf{t}}} \right]_0^{T_s} = \mathbf{h}_{\text{pu}} \left(1 - e^{-e\dot{\mathbf{t}}_s} \right)$$

Eq. 6

From this, the estimation of strain rate was made as an average over the experimental separation time, T_s , from the scaling factor, k , by,

$$k = \left(1 - e^{-e\dot{\mathbf{t}}_s} \right)$$

Eq. 7

As we see later, the asymptote of extension during the rise time of tack does, however, go effectively to infinity, such that the force-time integral over T_s in Eq. 6 is better approximated by Eq. 4, i.e. simply by \mathbf{h}_{pu} . [This is not expected to be the case once the time to tack maximum is exceeded - a subject for further study]. This negates only the approximate prediction previously held for $\dot{\mathbf{e}}$ but not the other conclusions.

Practically, L_0 is related to the reduced wet or effective mobile layer. However, the extension of the film is so great, leading in fact to a final fracture of the film, that the ratio L/L_0 is always assumed large over the extent of the pull-off action such that conditions of strong flow only are considered. For thicker layers and slower separation times the change to weak flow might be a complicating factor. There is

a further limitation in the integral assumption of Eq. 4 and Eq. 6, in that \mathbf{h}_{pu} is considered constant throughout the separation. As we shall see later, this is probably not the case in the light of the experimental analysis given in this new observation. However, if a time average regime is considered, as in fact is realistically included in the definition of the tack force itself, the scaling factor k that was used can be expected to make a good compensation for this assumption.

The development of the instrument to obtain position-sensitive data during the pull-off, to allow evaluation of \mathbf{e} and $\dot{\mathbf{e}}$, the work of tack, and potentially adhesion, and to illuminate the separation mechanisms, is now the subject of the experimental part of this paper.

EXPERIMENTAL METHOD

Ink-on-paper tack as measured by the ISIT device is defined as the maximum force experienced by a contact disc (tack wheel) of material similar to an offset printing blanket separating from a tackifying ink film, measured using a solenoid, coil spring and load cell (3). The ink film is applied from a printing disc pre-inked via an inking unit (IGT Reptest²). The total exposed roller area on the distributor was calculated to be 0.124 m². Typically an amount of 0.3 ml ink is applied by means of an IGT ink pipette. The distributor rotates at approximately 1 s⁻¹ (not adjustable) and the ink spreads over the exposed roller area by film-splitting with the print disc rotating with the main rubber roller. Subsequently, the print disc is manually transferred to the ISIT machine where the substrate strip is attached to the sample carrier with a double sided self-adhesive tape. The ISIT test cycle is started via a linked PC and in a revolution of the sample carrier the print disc transfers the ink to the paper.

The contact tack disc (or tack wheel) is then pressed against the print on the sample platen by the electromagnetic force acting on the solenoid. This action applies an extensional force on the coil spring mounted in parallel with the solenoid. Contact time and force can be varied by electronic controls to optimise adhesion between contact disc and print. At cessation of the electromagnetic force, controlled by the ramp-down function³, the contact disc is retracted from the print by the strain force of the extended coil spring, strong enough to achieve separation of the disc from the ink film. Under small extensions, the coil spring in combination with the chosen ramp-

² IGT Reptest B.V., P.O. Box 4672, 1009AR Amsterdam, The Netherlands, www.igt.nl

³ In this work, the ramp-down function is set to an exponential decay so as to ensure strong flow under extension.

down function provides a constant acceleration during the retraction of the disc. This is a unique feature of this static test procedure. The strain gauge, fixed between contact disc and coil spring, generates a load-dependent signal which is recorded as the force during separation as a function of time. The maximum in this force is defined as the tack force at the given time of separation. The sequence is automatically repeated for a pre-defined number of cycles chosen to span the timescale regions of the tack force under study. The build-up of the tensile force, $F(t)$, required to achieve each individual separation is recorded with time (pull-off curve) and can be analysed through specifically designed software.

Development of a laser-based strain sensor

To pursue observation of the physical displacement of the tack wheel during separation, $x_w(t)$, required a displacement sensor to monitor the position of the tack wheel as a function of time. A limiting factor was the mechanical tolerance of the ISIT components involved in the tack wheel motion. Conformation to an uneven substrate, such as paper, demands that the "play" in the tack wheel transverse mounting must be sufficient to ensure even deformation of the rubber offset blanket-like material on the tack wheel. This prevented an analysis of absolute position per se, but an assessment relative to the start position was possible to high accuracy, and this is what is needed for the definition of \mathbf{e} .

The requirements for the sensor were that it should work in a non-contact mode, it should fit dimensionally into/onto the apparatus, and have a practically achievable resolution of approximately 1 μm . The easiest and most economic approach was identified based on a laser cantilever method. The principle is shown in Fig. 2. The motion of the tack wheel is transferred via its extended axis to a thin connected mirror pivoting around a fixed base-point.

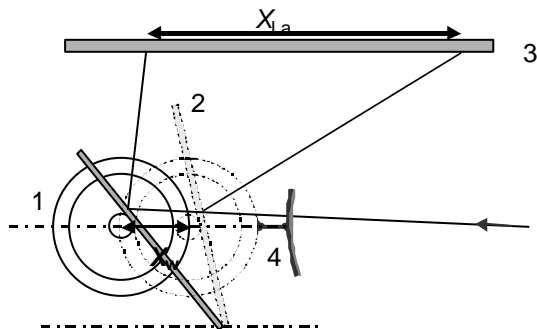


Fig. 2 Schematic of the laser cantilever: [1] tack wheel moving a distance x_w , [2] thin pivoting mirror guided by the extended axis of the tack wheel. The ray lines indicate the laser beam, [3] is the plane on which the projected laser dot motion is monitored by means of a high-speed camera, [4] represents the

printed paper strip with the ink-film being elongated into a lamellar filament (greatly exaggerated for clarity).

The experimental setup is shown in Fig. 3. All the parts used (obtained from Edmund Industrial Optics⁴ and Coherent⁵) are detailed in the Appendix. [The square brackets in the following description refer to Fig. 3]. The xz -table [1] consists of a precision 6.5" screw travel movement with an L-bracket mount. The mirror [2] consists of a microscope slide with a thickness of approximately 0.05 mm and a weight of 0.53 g. At first a gold-plated slide was used but an uncoated slide shows sufficient reflection and further provides a transmitted reference beam helpful in controlling the alignment of the system. The mirror is fixed via a sliding holder / adapter which was machined from aluminium, Fig. 4. The adapter has a clearance which permits the mirror a sliding motion, where friction was minimised by applying a thin layer of graphite. The most practical way to provide a pivoting point fulcrum was to use a household self-adhesive tape.

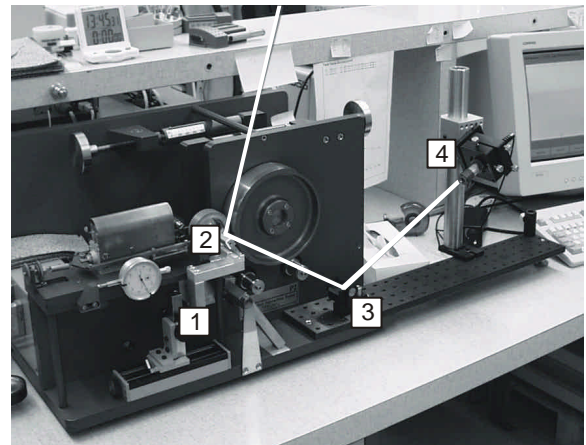


Fig. 3 The laser setup on the ISIT device (no ink or paper applied): [1] the xz -table holding the mirror, [2] tack wheel with extended axis pivoting the mirror, [3] beam steering unit and [4] diode laser. The laser beam is drawn schematically into the image.

⁴ Edmund Industrial Optics, 101 East Gloucester Pike, Barrington, NJ 08007-1380 USA

⁵ Coherent Auburn Group, Lindbergh Street, Auburn, CA 95602-9295 USA



Fig. 4 Detailed view of the mirror (glass slide) and the tack wheel; No.[2] in the previous figure.

The laser diode was mounted on a bench-plate using a mounting rod with carrier and an angle bracket. A beam steering unit [3], consisting of a mirror which is freely positionable in 3 dimensions, was used to reflect and guide the laser beam to the mounted mirror as shown in Fig. 3. The laser diode [4] has a circular beam diameter of 1.2 mm, a wavelength of 635 nm and a power of 4 mW, and is held by a 4-axis laser mount. The laser is powered by a Coherent LabLaser universal power supply.

The laser beam, reflected by the pivoting mirror, projects a path upwards toward the laboratory ceiling where a millimetre-scale graph paper is fixed, upon which the laser dot or point is observable.

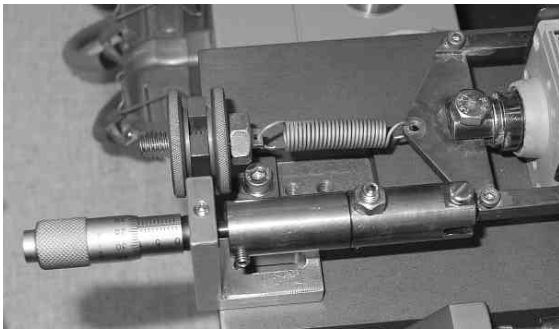


Fig. 5 Micrometer screw with adapter, used for the calibration of the ISIT tack wheel motion, is mounted in place of the coil spring in the picture.

The ratio of magnification from the micrometre displacement of the tack wheel to the recorded motion of the laser point was performed by direct mechanical calibration. A micrometer screw gauge (Mitutoyo, range 1 000 μm , precision 2 μm) was used to displace the tack wheel in increments of 50 μm (see Fig. 5). After each increment, the position of the laser point was marked on the millimetre graph paper. The marks were then measured manually using a vernier caliper. It is shown that an empirical linear function, as plotted and defined in Fig. 6, gives

a reasonable fit of the data points relating the two motions, i.e. that of the tack disc and that of the laser dot. Therefore, in this case, the transformation of the data between observed displacement on the millimetre scale and the actual tack wheel axis displacement can be made as follows:

$$x_w = (6.5922 x_{La} + 2.4389) \times 10^{-3}$$

Eq. 8

where x_{La} is the distance moved by the laser point and x_w is the displacement of the tack wheel, measured in the same units.

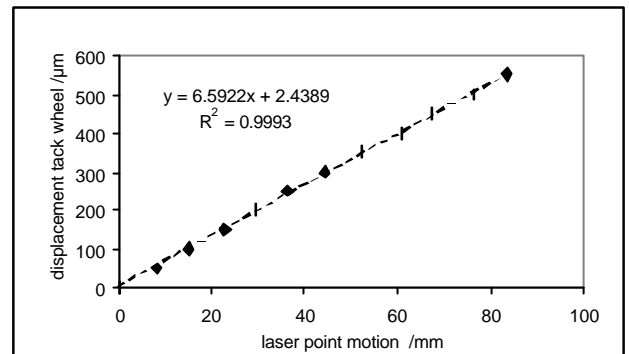


Fig. 6 Calibration of laser point to tack wheel displacement. 0 on the x-axis represents the point where the tack wheel touches the roll of the ISIT device. StdErr = 4.92 μm .

The motion of the laser dot was recorded with a high-speed camera, namely a MotionScope PCI 1000 from Redlake MASD Inc.⁶ A rate of 1000 frames per second and a shutter time of 1/2000 s were used. The recorded frames were analysed with the automated software package WINanalyse Motion Analysis⁷. This program detects the position of the marked features (here the laser point) in all of the captured frames, and provides for both 2D and 3D analyses on the sequence of images to derive additionally the velocity and acceleration of the dot, providing the angles of deflection between defined (marked) points of reference are known.

The calibration procedure was also carried out directly within the image analysis software by capturing the movement of the laser dot with the camera while displacing the tack wheel in increments using the micrometer screw gauge. The analysis was effectively calibrated directly by referring to the millimetre grid on the projection plane, without the need for the more generalised reference points, and shown to agree well with the manual scaling.

⁶ Redlake MASD Inc. San Diego, CA 92121-1097
www.redlake.com

⁷ Mikromak GmbH, am Wolfsmantel 18, D-91058 Erlangen, Germany, www.mikromak.com

Measurement procedure

The same commercial multicoated offset paper (Ikonofix⁸ 150 gm²) was used as in the previous tack experiments together with exactly the same instrumental settings and the same ink, Skinnex cyan 4x73⁹ (2). The sampling rate of the force values was enhanced by reducing "sample time" in the "system settings" menu from 50 ms to 10 ms. Three time points for the pull-off measurements were collected, namely after 1 s, 30 s (maximum tack) and 180 s (tack fall). Only the point at maximum tack was subsequently analysed here, where the ink is undergoing cohesive extension and a mixture of extension and ink-coating adhesion respectively. The time duration of the pull-off, T_s , was read from the individual force-time curves. The position of the laser point was recorded as a function of time as described in the previous section. The captured motion/time data were transferred from the software WINanalyse to MS Excel for scaling and plotting. The data for the distance displaced by the laser point during the pull-off was then transformed into x_w , the distance travelled by the tack wheel as shown in Fig. 7.

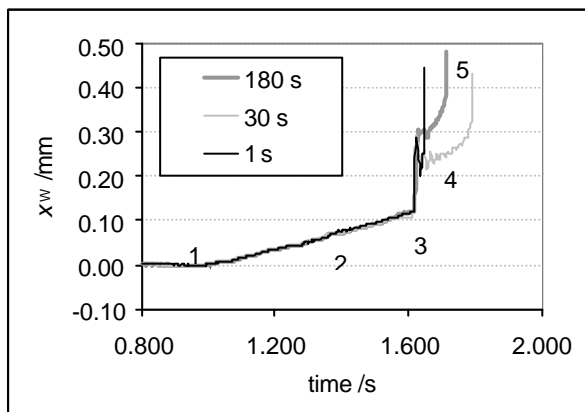


Fig. 7 The displacement of the laser point on the projection plane as recorded by the high-speed camera and transformed into x_w , the distance travelled by the tack wheel.

Clearly, different regimes are seen as denoted with the numbers 1-5 in Fig. 7. Careful observation of the tack wheel, and a short sequence recorded with the high-speed camera focussing on the wheel itself, revealed 1: the wheel being pressed against the paper strip, 2: the quasi-linear regime which is a manifestation of the decompression of the system (paper, adhesive tape and rubber of the tack wheel), confirmed by recording the action of the tack wheel separation in the absence of ink. Subsequently, 3: a transient of short and strong acceleration, followed by 4: an approximately exponential displacement

with some superimposed oscillations induced by the mirror, and finally 5: the definitive rupture and departure of the tack wheel.

Although the laser setup with the mirror yields a good resolution of the displacement of the tack wheel, the above mentioned oscillations complicated the analysis of separation rate at the shortest times (regime 4 in Fig. 7). Using an improved lens system on the high-speed camera, it was possible to focus directly on the edge of the tack wheel and capture the motion sufficiently precisely so as to smooth the data already obtained with the mirror.

An example of the smoothed recorded displacement is shown by the grey curve in Fig. 8, where the black curve represents the tack pull-off force-time curve for the same event. The excellent coincidence of the time spans of T_s , as represented by the tack pull-off curve and of the transient domains of the displacement curve, are immediately recognisable. This allowed us to unify the two graphs, i.e. to trigger to a common timescale with t set to zero at the transient point of tack rise and strain jump.

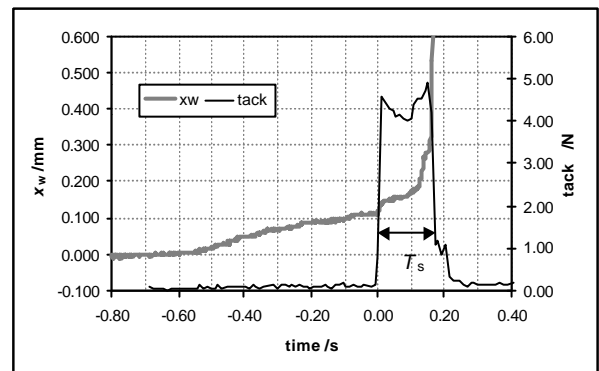


Fig. 8 Example of an ISIT pull-off curve (@30 s) superimposed on the displacement of the tack wheel.

The high resolution of the tack pull-off curve permits a closer inspection of the modes of tack wheel separation. We see that the separation from the thin printed ink layer is a two-step action. First of all, before separation, the compression of the rubber blanket-like material establishes a virtual parallel plate contact with the deformable paper substrate.

⁸ Ikonofix is a product name of Zanders Feinpapiere AG, D51439 Bergisch Gladbach, Deutschland

⁹ Skinnex is a product name of K+E Inks, Stuttgart, Germany

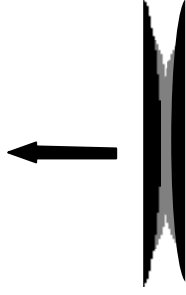


Fig. 9 Initial breakage of the film and formation of the free meniscus under extension is recorded as the first sub-maximum in the pull-off curve. The arrow indicates the separation movement of the tack wheel.

As the ramp-down in solenoid voltage begins, its form chosen by the user and controlled by the ISIT software, the spring acts to perform the separation of the tack wheel either through the ink film (at low tack) or from the ink film (after maximum tack). The initial separation occurs by the breakage of the film and retreat of the newly formed menisci toward the centre of the pull-off area (Fig. 9). This action predisposes the system ready to record the maximum tack force as would be seen by the separation of a printing blanket creating the free meniscus at the film split.

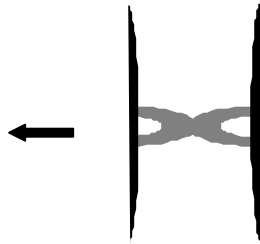


Fig. 10 Retreat of the menisci toward the centre and the formation of the lamellar filament. At maximum tack, adhesion failure may occur next to the paper. [Post tack adhesion should fail next to the blanket, if not then print rub can be suspected(4).]

After the retraction of the menisci to form a central planar (lamellar) filament (Fig. 10), the ink is further extended until finally the filament breaks. The pull-off area on the paper clearly shows the traces of the final lamellar filamentation either as a central line of higher print density or as a line of adhesion failure or sometimes pick. Normally, an extensional measurement in classical rheology concentrates on the continuous action of a free flowing material to describe the extensional strain rate. The action of blanket ink-split in practice, however, involves first the creation of the free meniscus. The extensional effect is therefore applicable strictly only as the elongation after film breakage, i.e. just prior to and during the filament lamella formation.

Coming back to Fig. 8, the two main-regimes discussed above can be recognised from the tack pull-off curve and are mirrored in the displacement curve of the tack wheel. The initial rate of change of position undergoes a slight vibration as the film is broken. The meniscus formation and rapid retreat is then determined as occurring over the separation time, T_s , starting from this initiating vibration. The transition between the two conditions occurs in the record of the tack for the given pull-off point. The inevitable elasticity in the mounting of the tack wheel results in a small momentum-driven overshoot of the wheel away from the mechanical withdrawing fork, shown as a short "rest period" on the distance-time plot, before the withdrawing fork once again tensions in contact with the tack wheel axis such that the controlled ramp-down of the solenoid voltage controls the continued extension of the filament under defined strain rate conditions. The force data collection continues to record the forces during the filament elongation, and they are seen to fall once again to zero at an effective infinite extension, thus satisfying the conditions for the theoretical force-time integral and the boundary conditions of the integral in Eq. 4.

RESULTS AND DISCUSSION

We can now go back to the earlier-made proposals for elongational flow and verify or otherwise the assumptions made in Eq. 2 - Eq. 7. We want to obtain a value for $\dot{\epsilon}$. From Fig. 8 we see that the initial assumption of constant acceleration (due to the exponential ramp-down) in the separation process seems to be correct. This means that we have so-called strong extensional flow.

Careful consideration is necessary to define what is meant by $(1/L)dL/dt$ as L and dL/dt are always changing. We therefore take the time average $\langle(1/L)dL/dt\rangle$, which is given by

$$\dot{\epsilon} = \left\langle \frac{1}{L} \frac{dL}{dt} \right\rangle = \frac{1}{T_s} \int_0^{T_s} \frac{\dot{x}_w(t)}{x_w(t)} dt$$

Eq. 9

We now determine the experimental rate of change of strain, $\dot{\epsilon}$, from the graphs by fitting a simple exponential equation (Eq. 10) to the separation regime of the graph of x_w against time, using TableCurve2D¹⁰, namely

$$x_w(t) = x_0 e^{ct}$$

Eq. 10

such that

¹⁰ TableCurve is a product name of SPSS Inc

$$\dot{x}_w(t) = cx_0 e^{ct} \quad \text{Eq. 11}$$

and so

$$\dot{\epsilon} = \left\langle \frac{1}{L} \frac{dL}{dt} \right\rangle = \frac{1}{T_s} \int_0^{T_s} c dt = c \quad \text{Eq. 12}$$

The values obtained are compiled in Table 1.

As discussed above, regarding the earlier publication (2), a scaling factor k was used to relate viscosity to the tack force-time integral terms as measured on the ISIT. It was stated that this factor might be related via already known parameters, Eq. 7, to obtain an estimate for $\dot{\epsilon} \approx 0.6 \text{ s}^{-1}$, for a pull-off time of $T_s \approx 0.2 \text{ s}$ and $k \approx 0.11$. The value of $\dot{\epsilon} = 50 \text{ s}^{-1}$ observed by the direct experimentation now presented is significantly larger. The problem most probably lies, as discussed in the Theory section, in the earlier definition of the relationship between the scaling factor k and $\dot{\epsilon}$, (Eq. 7) in which, as previously mentioned, h_{pu} is considered a constant in the integration when trying to extract the mechanical extensional dynamic and the extension was assumed to be non-asymptotic due to practical fracture of the ink rather than continued extension. We see that this is not the case for the region of tack rise where cohesive integrity is maintained.

Adj r^2=0.91946465 FitStdErr=2.0412111e-05 Fstat=949.21826
a=0.00015047129 b=1.111357e-07 c=48.103693

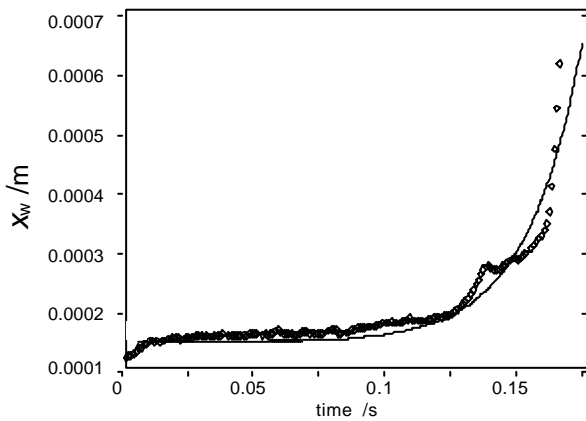


Fig. 11 A fit of Eq. 10 in the form of $x_w = a + b \exp(ct)$, where a is a simple start point shift constant and c is as given in Eq. 12.

This means that the integral in Eq. 6 gave a too small value for $\dot{\epsilon}$ in terms of k (Eq. 7). This does not invalidate the interpretation of the force-time integral in respect to dynamic viscosity, but does modify the description of the extension itself.

Furthermore, the asymptotic extension in combination with the falling separation force during final filamentation confirms that the ink shear thins and so the ink viscosity cannot be taken out of the integral in Eq. 6.

The work of tack measurement / separation, W_s , can now be calculated as the integrated tack force multiplied by the rate of displacement acting over the separation time, Eq. 13, i.e. force times displacement.

$$W_s \approx \int_0^{T_s} F(t) \dot{x}_w(t) dt \quad \text{Eq. 13}$$

To do this, since the separation force and displacement change with time, the tack force must be plotted against the corresponding displacement at each time point of the observation, i.e. the area under the curve of $F(t)$, defined during each single pull-off, against $x_w(t)$ must be obtained. In practice the curve cannot be integrated in all cases right up to T_s as the transient increase of x_w to the t asymptote is indeterminate. This is not because the data are unreliable but simply because we observe the motion of the wheel and assume the ink follows. This is true until the final break point, where the wheel continues to move under the defined ramp-down function but the ink clearly has passed its extension limit. The x_w data, therefore, past the tack force maximum are not usable to calculate the work done on the ink. This effectively influences only the last two data pairs from the merged curves in Fig. 8. The area under $F(t)$ against $x_w(t)$ was determined by fitting a function to the data points giving in each case an $r^2 > 0.98$ and then using the area function in TableCurve2D.

The values are reported in Table 1 where the work of tack measurement, i.e. separation of the tack wheel, is W_s (J), the specific work per unit line width of tack wheel contact, i.e. equivalent to unit line width of blanket contact, is defined as linear work W_{line} (Jm^{-1}) and the specific work per unit contact area W_{area} (Jm^{-2}), surface tack, is defined over the footprint area A_F ($= 51.7 \text{ mm}^2$).

The work so described enables a deeper discussion of Eq. 1 especially in terms of the energy required to form free surface, contained in F_m and related to ink surface tension, the viscous deformation/extension, F_η , and adhesion force, F_{ad} .

Elapsed time of pull-off point after printing /s	1	30	180
Time of separation T_s /s	0.12 ± 0.01	0.18 ± 0.02	0.09 ± 0.00
Max. tack force /N	3.76 ± 0.21	4.98 ± 0.26	2.21 ± 0.35
Force-time integral /Ns	0.36 ± 0.03	0.94 ± 0.13	0.17 ± 0.01
Measured parameters reported at maximum tack (elapsed time 30 s only)			
Measurement no.	1	2	3
Strain rate $\dot{\epsilon}$ /s ⁻¹	50.6	48.1	44.7
Work of tack measurement W_s /mJ	0.37	0.99	0.85
Work of linear tack W_{line} /Jm ⁻¹	0.02	0.06	0.05
Surface work of tack W_{area} /Jm ⁻²	7.2	19.2	16.5

Table 1 Overview of data and results

SUMMARY AND CONCLUSIONS

A direct measurement technique has been developed to view the separation dynamic of a blanket-like material from a printed paper during ink setting. This was achieved by an optical device mounted on an Ink-Surface Interaction Tester (ISIT) and recorded by a high speed camera.

The technique provides a first confirmation of an extensional model which describes reasonably well the tack force generation in terms of uniaxial viscous extension. This supports the proposal that the viscous force term is the most important during separation, given the boundary conditions of a thin layer of ink and a microrough, permeable paper. However, within this force under elongation are both the surface tension (formation of new surface) and adhesion.

The value of uniaxial rate of change of strain, $\dot{\epsilon}$, was determined in the experiment to be $\sim 50 \text{ s}^{-1}$. That this differed considerably from the previously predicted value (2) is most probably accounted for by the realisation that the elongation is made under defined strain and not governed by the ink stress. Under these conditions the work of tack measurement, the linear tack energy per unit line width and the areal energy

can be determined. In cases of adhesion failure, this is a direct measure of adhesion energy - surface tension difference between the ink and the substrate.

The result has important implications for the definition of ink rheology in-situ on paper during tackification as it can give unique information about the empirical "shortness" of an ink during the print process and the affinity of the ink for the surface (adhesion). Such properties describe the empirical length to which a volume of ink (or any paste) can be drawn into a filament before it breaks - the typical printer's action of drawing a blob of ink out between two fingers - and the "stickiness" of that ink. Such "finger tests" are still used by the print expert as an important practical parameter to describe the viscoelastic relaxation characteristic of an ink. It is the aim of subsequent study to investigate this last issue in the region of tack fall and in the wider context of other liquids and suspensions applied to various permeable substrates.

Acknowledgement

Thanks are given for the invaluable assistance given by Thomas Kozlik, Omya AG, during data collection, sample preparation and for many practical contributions.

APPENDIX

Parts, together with part numbers, used for the laser sensor:

Edmund Industrial Optics¹¹.
precision 6.5" screw travel movement L03-601
bench plate, L03-638

Coherent¹².
mounting rod, 61-1236,
carrier, 61-1509,
angle bracket, 61-1376,
beam steering unit, 22-8882,
laser diode, circular beam with a diameter of 1.2 mm,
a wavelength of 635 nm and a power of 4 mW

REFERENCES

- Desjumeaux, D. M. and Bousfield, D. W., "Modeling of ink film leveling with mobile phase removal", Pan-Pacific and International Printing and Graphic Arts Conference, October 6-8, 1998, Québec Canada, Pulp and Paper Technical Association of Canada, 1998, p103-109

¹¹ Edmund Industrial Optics, 101 East Gloucester Pike, Barrington, NJ 08007-1380 USA

¹² Coherent Auburn Group, Lindbergh Street, Auburn, CA 95602-9295 USA

2. Gane, P. A. C., Schoelkopf, J., and Matthews, G. P., "*Coating imbibition rate studies of offset inks: a novel determination of ink-on-paper viscosity and solids concentration using the ink tack force-time integral*", 2000 International Printing & Graphic Arts Conference, Savannah, GA, Tappi Press, Atlanta, 3-10-2000, p71-88
3. Gane, P. A. C. and Seyler, E. N., "*Some aspects of ink/paper interaction in offset printing*", Tappi Coating Conference Proceedings, 1994.
4. Gane, P. A. C., Seyler, E. N., and Swan, A., "*Some novel aspects of ink/paper interactions in offset printing*", International Printing and Graphic Arts Conference, Halifax, Nova Scotia, Tappi Press, Atlanta, 1994, p209-228
5. Macosko, C. W., "*Suspension Rheology*", Rheology: Principles, measurements and applications, VCH Publishers, New York, 1994, p425-474
6. Xiang, Y., Bousfield, D. W., Desjumaux, D., and Forbes, M. F., "*The relationship between coating layer composition, ink setting rate, and offset print gloss*", PanPacific and International Printing and Graphic Arts Conference, CPPA, 1998.